

The Method of Lines for the Analysis of Rectangular Spiral Inductors

F. J. Schmükle

Abstract—An accurate procedure is presented for the investigation of the electrical properties of rectangular spiral inductors. The models of the analyzed spiral inductors are composed of straight and bent multiple-line sections. The line sections are analyzed with the well-known Method of Lines (MoL). For the bends of coupled lines, a new analysis is used. The procedure considers all self- and mutual inductances of the straight multiple-line sections, as well as the electrical characteristics of the bends of coupled lines.

I. INTRODUCTION

IN monolithic integrated microwave circuits (MMIC's), rectangular coils are often required as passive elements with an inductive behavior at frequencies where quasi-TEM wave propagation can be assumed.

Many authors have treated the rectangular spiral inductors with different analyses. Most authors use models which consist of cascaded line sections, e.g., Cahana [1], Shepherd [2], Siegl [3], and Wiemer [4]. But some of these authors ignore electrical characteristics, which have an essential influence on the properties of the entire circuit; e.g., Siegl [3] neglects the electrical characteristics of the bends, and Cahana [1] neglects the negative mutual inductances between the lines of different spiral sides.

A recently presented coherent analysis from Djordjevic *et al.* [5] treats spiral inductors with 1 and 2 loops in "one piece." Hill and Tripathi [6] used the moment method for the calculation of the inductance of a spiral inductor. They modeled the inductance by dividing the spiral inductor with 1.75 loops into cascaded coupled (four port) transmission line sections, (four port) bends of coupled transmission lines, a single transmission line section, and bends of single transmission lines.

In the analysis described in this paper, the inductance is also modeled by subdividing the spiral inductor with N complete loops into cascaded transmission line bends with up to $N + 1$ lines and $2(N + 1)$ ports and coupled transmission line sections with up to $4(N + 1)$ ports. To consider the electrical characteristics of right angled coupled transmission line bends, a new approach [8], using the MoL, is applied. This new approach allows a high number N of lines in a comprehensive and accurate analysis of bends of coupled lines. For the analyses [7] of the coupled transmission line sections also, the well-known MoL is used.

Manuscript received December 30, 1991; revised November 2, 1992.

The author is with the Lehrstuhl für Allgemeine und Theoretische Elektrotechnik, Fern Universität, 5800 Hagen, Germany.

IEEE Log Number 9209341.

II. ANALYSIS

Two models are analyzed which differ in the treatment of the mutual inductances between the lines of different spiral sides. Both models consider the electrical characteristics of the multiple-line bends as analyzed in [8].

The first model (A) consists just of the series connected coupled transmission line sections (with up to $2(N + 1)$ ports), considering the self-inductances of the lines as well as the mutual inductances between the lines which belong to the same spiral side, but ignoring the mutual inductances between the lines of different spiral sides.

The second model (B) (Fig. 1) is composed of the coupled transmission line sections L3–L7 (with up to $4(N + 1)$ ports) and of the bends of coupled transmission lines E1–E4. In contrast to model A, all mutual inductances between lines of parallel spiral sides are also taken into account.

For the interconnection, the ABCD-matrices of all sections must be determined. By some simple extensions of the analyses used, the ABCD-matrices of the different multiple-line sections are easily derived. Owing to the equivalent ABCD-matrices of the bends E1, E2 and E3, E4, respectively (in the example of Fig. 1), it is sufficient to calculate the ABCD-matrices A_1 – A_7 . The interconnection of the ABCD-matrices for the example of Fig. 1 is shown in Fig. 2. The numbers in parentheses describe the input (1) and output (2) of each line

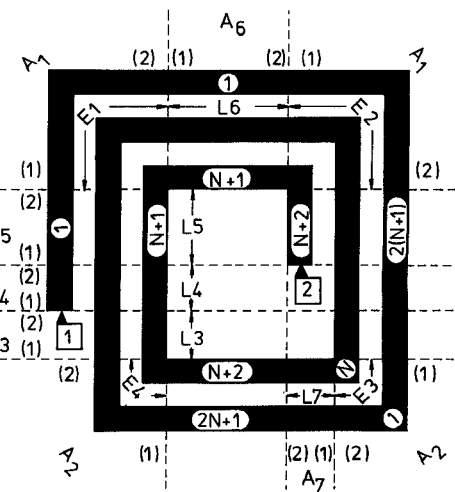


Fig. 1. Model of a spiral inductor with partitioning in straight and bent multiple line sections (e.g., the numbering of the lines of the sections L₅, L₆, and E₃ are outlined). L₃–L₇: straight multiple-line sections; E₁–E₄: bent multiple-line sections; A₁...A₇: assigned ABCD-matrices with input (1) and output (2) declaration.

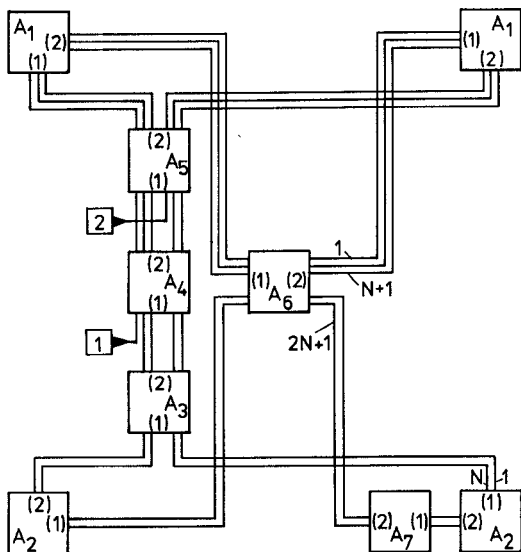


Fig. 2. Connections between the ABCD-matrices $A_1 \dots A_7$ for the spiral inductor in Fig. 1.

section corresponding to the equation

$$\begin{pmatrix} U_2 \\ I_2 \end{pmatrix} = A \begin{pmatrix} U_1 \\ I_1 \end{pmatrix} = \begin{bmatrix} A_{11} & A_{12} \\ A_{21} & A_{22} \end{bmatrix} \begin{pmatrix} U_1 \\ I_1 \end{pmatrix} \quad (1)$$

which connects the input and output quantities using the ABCD-matrix. From this arrangement, the ABCD-matrix of the spiral inductor related to its connections (1,2 in Fig. 2) is determined.

The arrangement and the sizes of the ABCD-matrices depend on the position of the connections (1,2 in Fig. 2) of the spiral inductor at the spiral sides to each other. The other possible arrangements are not explained, but they can easily be derived from the fundamental arrangement in Fig. 2.

For each spiral inductor, the simple equivalent circuit (Fig. 3) is used and its elements are determined from the ABCD-matrix of the complete circuit.

The described type of modeling spiral inductors by subdividing into cascaded sections is limited to structures with ratios of the smallest inner side length to the substrate thickness $l_s/h > 0.5$. For ratios beneath this value, the bends of coupled lines affects one each other, so that the assumptions do not hold.

III. RESULTS

Different spiral inductors have been investigated, using both models A and B explained in the last section. The results show

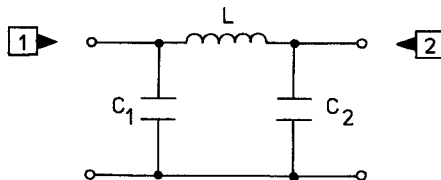


Fig. 3. Equivalent circuit of a spiral inductor.

that for the investigated ratios $0.5 < l_s/h < 3.0$, accurate values of the inductance cannot be determined from model A. At these ratios, the values of inductance are considerably affected by the effects of the bends of the coupled transmission lines, as well as of the mutual inductances between lines which belong to different spiral sides. Hence, in the following only, the results of investigations of some other authors, who consider at least the effects of the line bends, are compared to the results concerning models A and B.

The spiral inductor shown in Fig. 4 was investigated by Cahana [1], considering the effects of one-line bends (with the results of the investigations of Neale and Gopinath [9]), but neglecting the negative mutual inductances between the lines of different spiral sides, yielding the value of $L = 1.5nH$. The calculation of the spiral inductor in Fig. 5 gives $L = 1.45nH$ (model A) and $L = 0.9nH$ (model B). Owing to the sharp bends of the spiral inductor in Fig. 5, and to the neglect of the influence of the bend at the left connection of the spiral inductor in Fig. 4, the small difference between the result for model A and Cahana's model was expected.

Obviously, the result for model B deviates very much from both other results. As the substrate thickness is greater than the comparatively small diameter of the spiral inductors, strong negative mutual inductances between the lines of different spiral sides appear. These are considered in model B, but are neglected in model A and Cahana's model.

On the other hand, the results of Djordjevic *et al.* [5] (Table I) agree fairly well with those calculated with both models in this analysis. Using the finite element method, they analyzed a one-and a two-turn spiral inductor (Fig. 6), respectively, in one-step analyses of the entire structures. The results in the contribution of Djordjevic *et al.* [5] are rounded to the first decimal. This may explain the greater deviations between the results of the one-turn spiral inductors compared to those between the two-turn spiral inductors.

Owing to the small substrate thickness compared to the diameter of the spiral inductors, only little differences appear

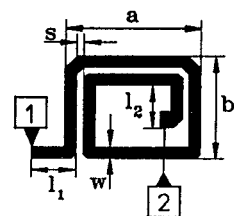


Fig. 4. Spiral inductor investigated by Cahana [1]. $a = 250 \mu\text{m}$, $b = 200 \mu\text{m}$, $w = 11.4 \mu\text{m}$, $s = 8.9 \mu\text{m}$, $h = 318 \mu\text{m}$, $l_1, l_2 = 152 \mu\text{m}$, $\epsilon_r = 12.9$.

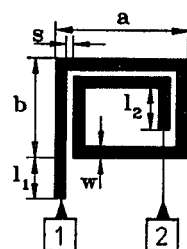


Fig. 5. Spiral inductor for comparison to Fig. 4.

TABLE I

Model	Inductance L in nH
A one-turn	1.58
B one-turn	1.55
Djordjevic <i>et al.</i> [5] one-turn	1.7
A two-turn	3.24
B two-turn	3.18
Djordjevic <i>et al.</i> [5] two-turn	3.3

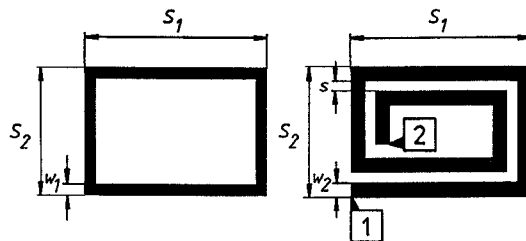


Fig. 6. One-turn and two-turn spiral inductor, investigated by Djordjevic *et al.* [5]. $w_1 = 300 \mu m$, $w_2 = 250 \mu m$, $s_1 = 2500 \mu m$, $s_2 = 2000 \mu m$, $s = 150 \mu m$, $h = 100 \mu m$, $\epsilon_r = 1.0$.

between the results for models A and B. Therefore, the effects of the negative mutual inductances between the lines of different spiral sides can be neglected here.

For a 3.25-turn spiral inductor with slotwidth s = stripwidth $w = 20.0 \mu m$, an outer sidelength of $360.0 \mu m$ on a $200.0 \mu m$ -thick substrate with $\epsilon_r = 12.9$, Shepherd [2] calculated a value of inductance of $L = 3.0nH$. With the presented procedure, using the MoL, an inductance of $L = 3.2nH$ was calculated (model B).

For 1.25-, 1.75-, 2.0-, and 2.5-turn spiral inductors, Figs. 7, 8, and 9 show the values of inductance for varying substrate thickness h , ratios s/w of slotwidth to stripwidth, and inner side lengths l_i , calculated with the described analysis.

Owing to the minor field coupling between the lines of different spiral sides at comparatively high ratios of l_i/h , the negative mutual inductances are also small. Therefore, the values of inductance for both models must approach with decreasing substrate thickness, which is proved by the behavior of the curves in Figs. 7 and 9. At low ratios of l_i/h (Fig. 9), the relative deviation between the values of both models increases because of the stronger influence of the negative mutual inductances.

Additionally, the electrical characteristics of the bends of coupled lines lead to decreasing values of inductance for increasing substrate thickness. For small ratios $w/h < 0.2$ of stripwidth to substrate thickness, the effect of one bend of coupled lines onto the inductance is comparable to a shortening of each connected spiral side by more than 15% of the substrate thickness in the investigated cases.

For a spiral inductor (Fig. 9) with $h = 635 \mu m$, $l_i = 550 \mu m$, and a square metallization of $200 \mu m$ side length in the center of the inductor, a measurement yields the value $L \approx 6.4nH$. This value lies between the results for model A and model B, the deviation to the value of model B is explained by the effect of the square metallization.

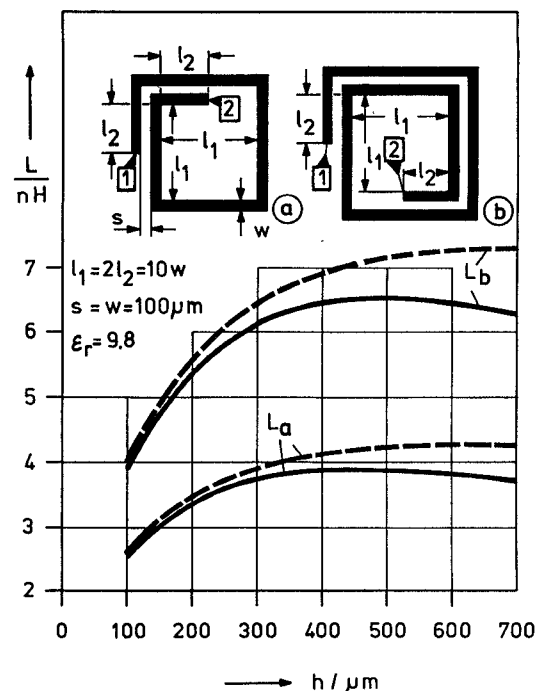


Fig. 7. Values of the series inductance of a 1.25- and a 1.75-turn spiral inductor versus the substrate thickness h . Model A: ---; Model B: —.

IV. CONCLUSION

An accurate procedure, based on the Method of Lines, was presented for the analysis of rectangular spiral inductors. The procedure considers all self- and mutual inductances of the straight multiple-line sections, as well as the electrical characteristics of right angled bends of coupled lines.

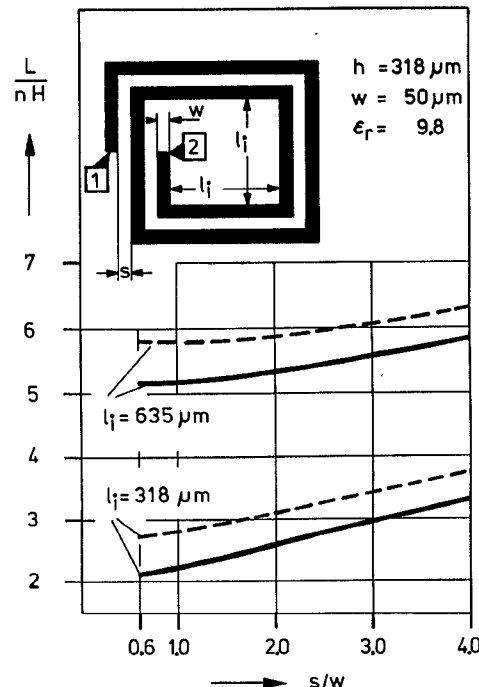


Fig. 8. Values of the series inductance of a 2.0-turn spiral inductor versus the ratio s/w from slotwidth to stripwidth for different inner side lengths l_i . Model A: ---; Model B: —.

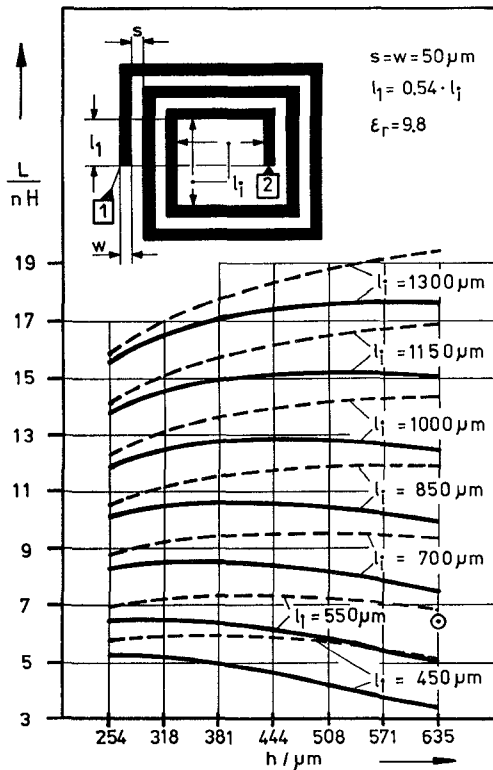


Fig. 9. Values of the series inductance of a 2.5-turn spiral inductor versus the substrate thickness h for different inner side lengths l_i . Model A: $---$; Model B: $—$. \odot : comparing measurement of a spiral inductor with $h = 635 \mu\text{m}$; $l_i = 550 \mu\text{m}$; and a centered square metallization of $200 \mu\text{m}$ side length.

ACKNOWLEDGMENT

The author gratefully acknowledges the great help from Prof. Dr.-Ing. R. Pregla of the Institut für Allgemeine und

Theoretische Elektrotechnik at the Fern Universität, Hagen, Germany, who gave the initial ideas, as well as from the Volkswagenstiftung, Germany, which promoted this project.

REFERENCES

- [1] D. Cahana, "A new transmission line approach for designing spiral microstrip inductors for microwave integrated circuits," in *Int. Microwave Symp. IEEE Trans. Microwave Theory Tech.-S Dig.*, pp. 245–247, 1983.
- [2] P. R. Shepherd, "Analysis of square-spiral inductors for use in MMIC's," *IEEE Trans. Microwave Theory Tech.*, vol. MTT-34, pp. 467–472, 1986.
- [3] J. Siegl, "PLANAR—ein Programm zur Simulation von Hochfrequenzschaltungen mit verteilten Leitungstrukturen," *FREQUENZ*, vol. 40, pp. 209–214, 1986.
- [4] L. Wiemer, "Interdigitale und spiralförmige Komponenten planarer Technologie in monolithisch integrierten Mikrowellen-Schaltungen," Ph.D. dissertation, Universität -GH- Duisberg, FRG, 1988.
- [5] A. R. Djordjevic, C. K. Allen, T. K. Sarkar, and Z. A. Maricevic, "Inductance of perfectly conducting foils including spiral inductors," *IEEE Trans. Microwave Theory Tech.*, vol. MTT-38, pp. 1407–1414, 1990.
- [6] A. Hill and V. K. Tripathi, "Analysis and modeling of right angle microstrip bend discontinuities," in *IEEE MTT-S Dig.*, 1989, pp. 1143–1146.
- [7] R. Pregla and W. Pascher, "The Method of Lines," in *Numerical Techniques for Microwave and Millimeter-Wave Passive Structures*, X. Itih, Ed. New York: Wiley, 1989, pp. 381–446.
- [8] F. J. Schmükle, "The method of lines for the rigorous analysis of rectangular bends of multiple-line-systems," in preparation.
- [9] B. Neale and A. Gopinath, "Microstrip discontinuity inductances," *IEEE Trans. Microwave Theory Tech.*, vol. MTT-26, pp. 827–831, 1978.
- [10] R. Garg and I. J. Bahl, "Microstrip discontinuities," *Int. J. Electron.*, vol. 45, no. 1, pp. 81–87, 1978.

F. J. Schmükle, photograph and biography not available at the time of publication.